ELSEVIER

Catalysis Today 38 (1997) 467–472

CATALYSIS TODAY

Development of novel anodes for solid oxide fuel cells

J.T.S Irvine[a,*], D.P. Fagg[b], J. Labrincha[c], F.M.B. Marques[c]

[a] *School of Chemistry, University of St Andrews, St. Andrews, Fife KY16 9ST, UK*
[b] *Department of Chemistry, University of Aberdeen, Aberdeen AB9 2UE, UK*
[c] *Department of Ceramics and Glass, University of Aveiro, Aveiro 3800, Portugal*

Abstract

Ni cermet anodes pose considerable problems for SOFC operation in natural gas fuels, particularly with regard to carbon deposition due to hydrocarbon cracking. Oxide anodes offer a good alternative, particularly if a material combining good electronic and ionic transport properties can be utilised. In our search for alternative anode materials, we have investigated fluorite-based systems containing reducible early transition metal dopants. The extent of phase stability has been investigated by solid-state chemical techniques and electrical properties have been investigated by ac impedance techniques as a function of both temperature and oxygen partial pressure. The Nb–Zr–Y–O system has been found to provide a good model system exhibiting reasonable electrical properties. Niobium pentoxide exhibits a wide range of solid solubility in the yttria–zirconia cubic fluorite system and the fluorite structure is retained under reducing conditions. Electronic conductivity increases as niobium concentration increases; however oxide–ionic conductivity decreases with extent of niobium substitution. The defect chemistry of this system, which determines the electrical properties, is dominated by the high concentration of oxide vacancies necessary to stabilise the cubic structure, hence electronic conductivity exhibits a $p(O_2)^{-1/4}$ dependence on oxygen partial pressure. © 1997 Elsevier Science B.V.

1. Introduction

Fuel cells offer a means of electrochemical conversion of either hydrogen or hydrocarbon fuels to energy. One of the most promising designs of fuel cell is the solid oxide fuel cell (SOFC), which is an all ceramic device that operates at temperatures in the 850–1000°C range [1]. This design holds particular promise for power generation, particularly for combined heat and power operation [2]. Although there is some interest in lower temperature modifications, most current development centres on designs based on the yttria-stabilised zirconia electrolyte, with (La,Sr)MnO_3 as the preferred cathode and Ni/ZrO_2 cermets as the preferred anode [3]. In this article we address the optimisation of anodes for operation in natural gas fuel.

The requirements for efficient anode operation are many, so the search for alternative materials is not a simple task. Anode materials must be stable both at the low oxygen partial pressures prevalent in the fuel gas and at the more oxidising conditions at the fuel outlet. Anodes must exhibit suitable catalytic and electrical properties and they must also be structurally and mechanically compatible with the electrolyte up to operating temperatures (at 1000°C).

Ni/ZrO_2 cermet anodes are inexpensive and, as Ni exhibits high catalytic activity for hydrogen oxidation

---

*Corresponding author.

0920-5861/97/$32.00 © 1997 Elsevier Science B.V. All rights reserved.
PII S0920-5861(97)00056-4

[4], these materials have been widely utilised in SOFCs with hydrogen fuel. The Nickel loading is generally chosen to be slightly in excess of the limit for percolation electronic conduction [3]. At higher Ni loadings there are problems with thermal expansivity mismatch between the Ni and the zirconia electrolyte substrate [5]. The major disadvantage of the Ni cermet electrode arises from the promotion of competitive catalytic cracking of hydrocarbon reactions [6]. The rapid deposition of carbon at Ni cermets means that direct oxidation of methane is not technically viable in solid oxide fuel cells. In order to utilise methane as fuel in SOFCs, the fuel needs to be reformed with steam either externally or internally [6].

The reforming reaction (1) is generally associated with a following water gas shift equilibrium reaction (2):

$$CH_4 + H_2O_{(g)} \Leftrightarrow CO_{(g)} + 3H_{2(g)} \qquad (1)$$

$$CO_{(g)} + H_2O_{(g)} \Leftrightarrow CO_{2(g)} + H_{2(g)} \qquad (2)$$

Both these reactions are favoured by low pressures and high temperatures and by large steam partial pressures. If insufficient steam is present, carbon may be deposited according to reaction (3).

$$CH_{4(g)} \Leftrightarrow C_{(s)} + 2H_{2(g)} \qquad (3)$$

This cracking reaction is even more problematic with higher hydrocarbons, which are also present in natural gas. External reforming requires a major cost addition to the plant required for SOFC operation and so is not an attractive option. There is a considerable research effort to build SOFC stacks which reform internally [7], although there are still major problems to be overcome including temperature gradients across the cell anode. These arise because the reforming reaction, which occurs rapidly at Ni is endothermic, whereas the oxidation reactions are exothermic. One further problem for utilisation of natural gas at Ni cermet anodes is sulphur intolerance [8], resulting in the deposition of nickel sulphide at the anode. In addition, sintering of Ni on prolonged operation is a potential problem for any type of fuel [9].

Transition metal-oxide anodes promise considerable improvements over Ni cermets in relation to most of the problems discussed above. The primary advantage of transition metal oxides is the accessibility of multiple oxidation states (Eq. (4)).

$$M^{4+}O_{n/2}/M^{(n-1)+}/\ldots/M^{+}O_{0.5}/M \qquad (4)$$

The accessibility of mixed valence states facilitates electronic conductivity and generally enhances catalytic activity. Under operating conditions, i.e., $T \rightarrow 1000^\circ C$, catalytic activity for fuel oxidation is not likely to be a limiting factor for most transition metal oxides, though the relative catalytic activities for oxidation and cracking are more important. If the metal is selected so as to ensure that a lower oxide, as opposed to the metal, is stable under fuel electrode conditions, cracking reactions are likely to be retarded due to the availability of surface oxygen.

One particularly attractive approach is the development of mixed conducting oxides as electrodes. In these oxides, both electrons and oxide ions exhibit high mobilities, so that the electrochemical reaction can occur at the electrode/gas interface as opposed to the three-point contacts between electrode, electrolyte and gas [10], Fig. 1. If suitable anodes, or cathodes, can be developed which combine this greatly enhanced catalytic activity with good stability, then significant improvements in fuel cell efficiency can be achieved.

Oxides with the fluorite structure are well known for their high oxide-ion conductivity and good thermal stability. Fluorite oxides are also readily substituted by early transition metals, facilitating electronic conductivity. In this paper, we discuss some of our recent

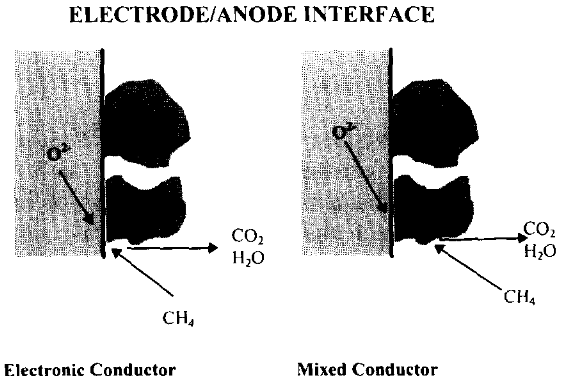

Electronic Conductor **Mixed Conductor**

Fig. 1. Schematic diagrams of oxidation reactions occurring at electronic and mixed conducting electrodes Charge transfer occurs at the electrolyte–anode-gas boundary for the electronically conducting anode, whereas charge transfer can occur anywhere on the surface of the mixed conducting anode.

investigations of early transition metal substituted stabilised zirconias concerning the Nb substituted yttria-stabilised zirconia system.

2. Experimental

Yttria (Aldrich), niobia (Aldrich) and zirconia (Tioxide) powders of purity 99.99%, were used as the starting materials. To prevent moisture and absorption of various gases, it was found to be necessary to dry Y_2O_3 for 24 h at 1000°C and to weigh directly from a desiccator. ZrO_2 and Nb_2O_5 were both dried at 700°C for 24 h. Stoichiometric amounts of these powders were thoroughly ground under acetone, using an agate pestle and mortar and pressed into pellets (8 mm × 3 mm) at a pressure of 3 ton/cm^2. The pellets were held at 1000°C for 3 h before being sintered at 1500°C for 32 h, or 1450°C for samples close to the Y_2O_3–Nb_2O_5 join. After sintering the pellets were removed from the furnace and rapidly cooled to room temperature. Phase purity was examined and unit-cell parameters determined using a Stoe Stadi-P diffractometer. For electrical measurements an organo-platinum paste was applied to each face of the pellets and fired at temperatures up to 1000°C. Measurements were performed in a controlled oxygen partial pressure furnace. This furnace utilised an yttria-stabilised zirconia oxygen pump to control oxygen partial pressure, with a separate oxygen sensor (yttria-stabilised zirconia) being utilised to monitor oxygen partial pressure [11–13]. Initially the furnace was purged with argon, then residual oxygen was pumped out of the furnace electrochemically. The pump was then switched off and oxygen allowed to diffuse back in over a period of ≈20 h. Total pressure was always close to 1 atm EMF measurements were generally taken on increasing oxygen partial pressure, whereas conductivity measurements were performed on both increasing and decreasing oxygen partial pressures. For EMF measurements, the sample was placed between an air atmosphere and the controlled oxygen partial pressure atmosphere. Electrical conductivity was measured at an ac frequency of 10 kHz, as oxygen partial pressure was allowed to vary. The data obtained at this frequency was found to agree within 2% to the values obtained from a full ac impedance scan under both the most oxidising and most reducing conditions used in this study. The 10 kHz point was found, at all $p(O_2)$ values to lie close to the intercept between bulk and electrode responses in complex impedance plots. Thus, the imaginary, Z'' value at 10 kHz was close to zero and the real, Z' value corresponded to the grain resistivity. The grain boundary component was negligible compared to the bulk at 1000°C.

3. Results and discussion

The range of the cubic zirconia solid solution for the niobia–yttria–zirconia solid solution has been determined in this study and is shown in Fig. 2. Phase limits on the ZrO_2–Y_2O_3 binary join are 15 mol% $YO_{1.5}$ and 55 mol% $YO_{1.5}$, in reasonable accord with the published phase diagram of Scott [14]. Above 55%, lines characteristic of the C-type structure of Y_2O_3 appear in the X-ray powder pattern. On the $YO_{1.5}$–$NbO_{2.5}$ binary join the limits of the cubic fluorite solid solution are 21 and 27 mol% $NbO_{2.5}$, in accord with the values reported by Bondar et al. [15]. Unit-cell parameters show a strong dependence upon yttrium content, increasing the unit-cell edge with substitution, as might be expected from ionic radius considerations. Nb^V is much better matched to Zr^{IV}, with only a slight decrease in unit-cell edge on Nb substitution (Fig. 3).

Two solid solution series were chosen to investigate electrical properties as a function of composition:

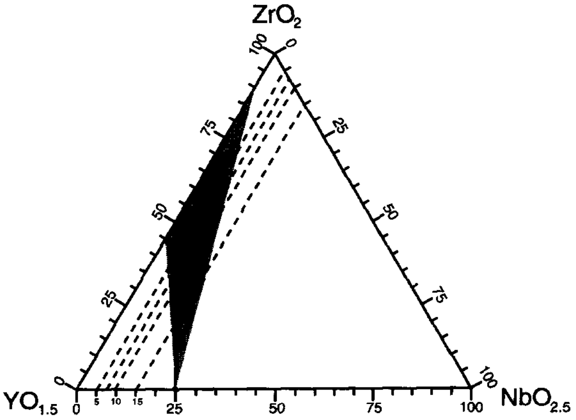

Fig. 2. Diagram of Y_2O_3 : ZrO_2 : Nb_2O_5 system showing extent of single-phase cubic solid solution region at ca. 1500°C, points correspond to samples investigated in conductivity studies.

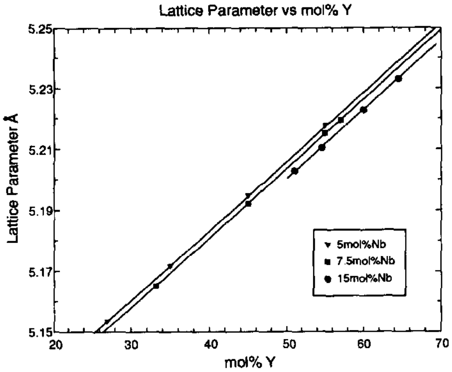

Fig. 3. Cubic unit-cell parameter, *a*, as a function of Nb and Y content in the solid solution $Nb_xY_yZr_{1-x-y}O_{2+(x-y)/2}$; lines join data points of equal Nb concentration.

A $Y_{2+x}Zr_{2-2x}Nb_xO_7$ and

B $Y_{0.6+2.4x}Zr_{3.4-3.4x}Nb_xO_{7.72-0.72x}$

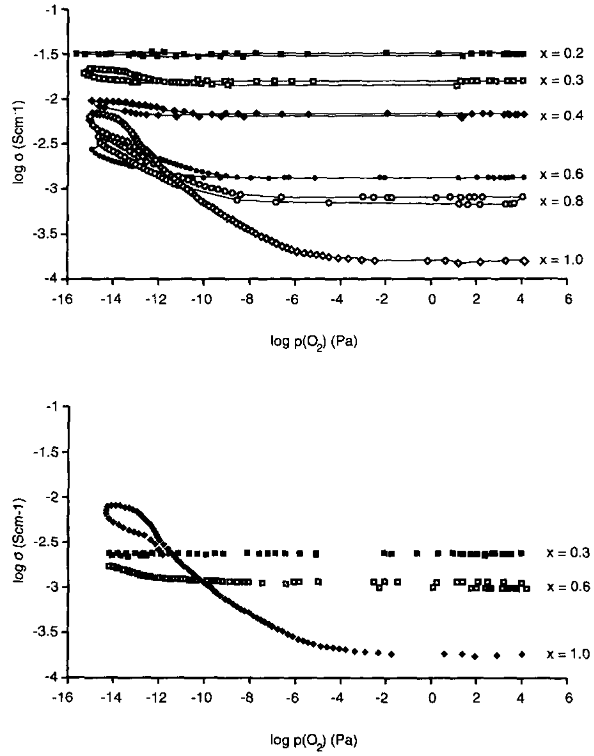

Fig. 4. Conductivity measured at 10 kHz and 1000°C as a function of oxygen partial pressure for (a) – $Y_{2+x}Zr_{2-2x}Nb_xO_7$, and (b) – $Y_{0.6+2.4x}Zr_{3.4-3.4x}Nb_xO_{7.72-0.72x}$.

These solid solutions occur close to the high-yttria and low-yttria limits of the cubic fluorite solid solution area and share a common end-member, Y_3NbO_7. Electrical conductivity data are presented in Fig. 4a and b. At low concentrations of Nb, conductivity is invariant of oxygen partial pressure, whereas at higher Nb concentrations an increase in conductivity is observed at low partial pressures of oxygen ($<10^{-5}$ Pa). This behaviour is indicative of mixed conductivity at low oxygen partial pressures. At high oxygen partial pressures, oxide-ion transport dominates conductivity; however, at low oxygen partial pressures, *n*-type semiconductivity induced by oxygen loss also contributes to conductivity. This suggestion is confirmed by the results from EMF measurements, e.g. Fig. 5, which show that the observed EMF correspond to the Nernst value over a wide range of oxygen partial pressures, indicating an ionic-transport number of unity. The EMF of most samples deviated from the ideal value at ca. 0.9 V (vs. air), or 10^{-10} Pa O_2, but even at the lowest partial pressures investigated the ionic-transport number remained above 0.8. The only exception was for Y_3NbO_7, where the electronic contribution to conductivity was about 30-times greater than the oxide-ionic contribution and so the ionic transport number dropped towards zero at the lowest oxygen partial pressures. In the experiments shown in Fig. 5, there is a deviation from linear Nernst behaviour at EMF values of approx. 0.4 V; this arises from the poor response kinetics of the sensor in this oxygen partial pressure range and is not attributable to any physical phenomenon in the material.

In both solid solution series the ionic contribution to conductivity, as indicated by the plateaux in conductivity values at high $p(O_2)$, decreased by one to two orders of magnitude as the degree of substitution increased. This is in accord with ac impedance studies performed in air [16]. Total conductivity also generally decreased with degree of substitution, although at the lowest oxygen partial pressures, conductivity did increase slightly with degree of substitution for niobium rich samples (Fig. 4a).

In mixed conducting samples two independent mechanisms of charge transport can be considered, involving oxygen vacancy migration and electronic hopping, i.e., assuming a parallel pathway. On sub-

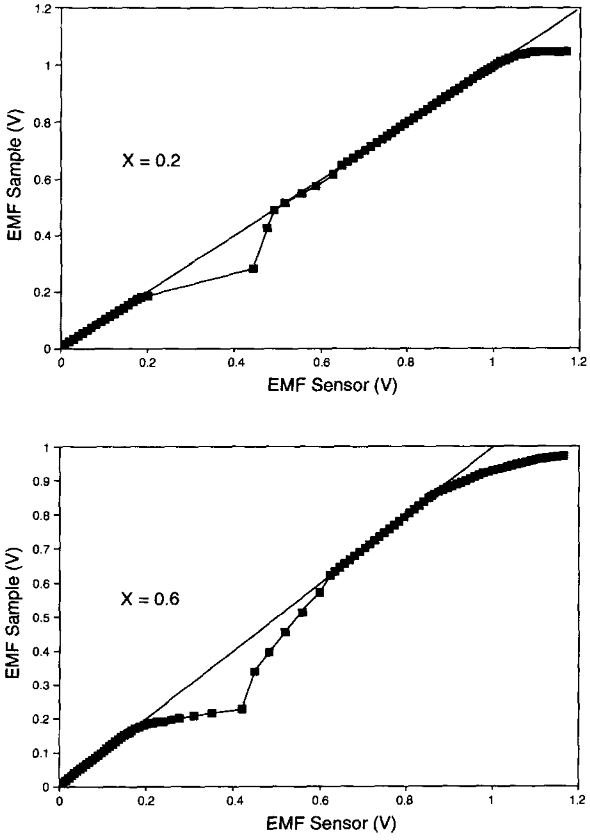

Fig. 5. EMF vs. air measured in a concentration cell for two samples in the series A $Y_{2+x}Zr_{2-2x}Nb_xO_7$, $T = 1000°C$. Data are plotted against the observed EMF of an yttria-stabilised zirconia oxygen sensor monitoring oxygen partial pressure.

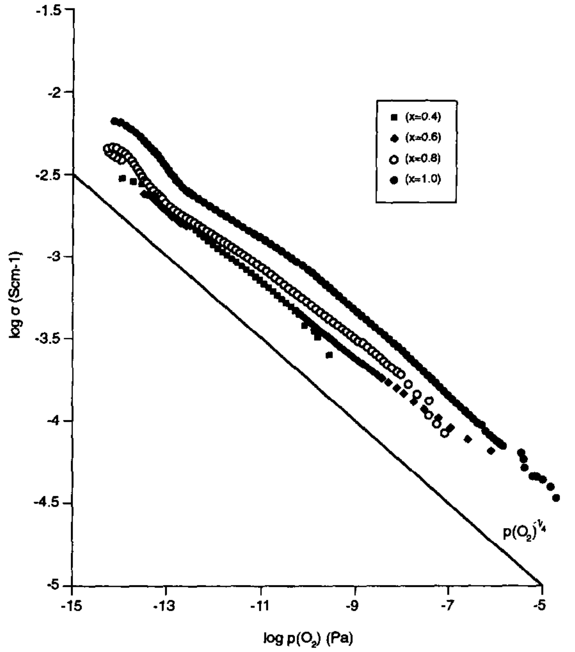

Fig. 6. Electronic contribution to conductivity as a function of oxygen partial pressure for $Y_{0.6+2.4x}Zr_{3.4-3.4x}Nb_xO_{7.72-0.72x}$, $T = 1000°C$ (the ionic contribution has been subtracted).

tracting the ionic contribution to conductivity, which is assumed to be independent of oxygen partial pressure, from the total conductivity the residual value corresponds to the electronic conductivity. The electronic conductivity thus obtained shows a simple dependence upon oxygen partial pressure (Fig. 6). Electronic conductivity increases with degree of substitution and shows a $p(O_2)^{-1/4}$ dependence. This is a fairly common defect chemical relation observed in oxides where the concentration of ionic carriers remains effectively constant as oxygen partial pressure is varied [13]. The generation of carriers in this system must be due to the reduction of Nb^V species on zirconium sites ($Nb^{\bullet}_{Zr}$) to Nb^{IV} species (Nb^{x}_{Zr}). The defect reaction is expressed, in Kröger–Vink notation, as:

$$Nb^{\bullet}_{Zr} + \tfrac{1}{2}O^{X}_{O} \Leftrightarrow \tfrac{1}{2}V^{\bullet\bullet}_{O} + Nb^{x}_{Zr} + \tfrac{1}{4}O_2 \qquad (5)$$

and, hence, the equilibrium constant for this reaction is given by

$$K = \frac{a^{1/2}_{V_O^{\bullet\bullet}}\, p(O_2)^{1/4}[Nb^{x}_{Zr}]}{a_{Nb^{\bullet}_{Zr}}\, a^{1/2}_{O^{x}_{O}}} \qquad (6)$$

If one assumes that the number of oxygen vacancies induced by reduction are much less than the number arising from the aliovalent substitution of yttrium for zirconium, then the only variables in Eq. (6) are the oxygen partial pressure and the number of Nb^{IV} species in the lattice. Therefore, the number of electronic carriers is given by:

$$n = [Nb^{X}_{Zr}] \propto pO_2^{(-1/4)} \qquad (7)$$

and, as mobility would be expected to be invariant with oxygen partial pressure in this system, the electronic conductivity is given by:

$$\sigma_e \propto pO_2^{-1/4} \qquad (8)$$

As this corresponds to the observed result, it seems clear that the number of oxide vacancies introduced on reduction does not significantly perturb the number of oxide ions available for migration. This is not surprising as thermogravimetry indicates that even in samples with the highest niobium content, much less than 1% of the oxide ions can be removed on reduction and the systems investigated all contain very high concentrations of oxygen vacancies.

4. Conclusions

Compositions from the fluorite solid solution system Y–Zr–Nb–O exhibit good structural and chemical compatibility with yttria-stabilised zirconia solid electrolytes and are resistant to chemical or structural changes on reduction. Electronic conductivity is induced in Nb-rich compositions on reduction; however, the conductivity values are only moderate, namely 10^{-2} S cm^{-1} at 1000°C. This is some five orders of magnitude lower than the conductivity of Ni/ZrO_2; however, much poorer conductivities than that of Ni/ZrO_2 could be tolerated without significant decrease in efficiency. On comparison with the conductivities of other fuel cell components [17] and allowing for possibility of using a dense electrode, a value of 1 S cm^{-1} seems a more appropriate target, although this is still nearly two orders of magnitude higher than the observed value in this system. The low electronic conductivity observed under reducing conditions may relate to the difficulty of removing oxygen from the lattice. It would seem that Nb^V is stabilised in the high vacancy content cubic fluorite lattice.

Ionic conductivity decreases on increasing Nb-content; however, even the lowest ionic conductivity values observed, 10^{-3} S cm^{-1}, should impart sufficient oxide ionic mobility to allow fuel oxidation to occur over the electrode surface, not just at three-point boundaries.

Niobium substituted yttria stabilised zirconia offers several features attractive for its use as an anode in solid oxide fuel cells; however, its low electronic contribution means that it is only likely to utilised in a commercial solid oxide fuel cell as part of a composite material. The system does offer a good model system whose electrocatalytic activity for hydrocarbon oxidation merits testing.

Acknowledgements

The authors acknowledge the support of British Gas Plc, in the form of a Research Scholarship (DPF), and the British Council/JNICT for a Treaty of Windsor award.

References

[1] B.C.H. Steele, Mat. Res. Bull. 14 (1989) 19.

[2] D.S. Beishon, M.R. Taylor, UK Department of Industry Report, ETSU/FCR/008.

[3] N.H. Minh, J. Am. Ceram. Soc. 76 (1993) 563.

[4] T. Setoguchi, K. Okamoto, K. Eguchi, H. Arai, J. Electrochem. Soc 139 (1992) 2875.

[5] D.W. Dees, T.D. Claar, T.E. Easler, D.C. Fee, F.C. Mrazek, J. Electrochem. Soc. 134 (1987) 2141.

[6] B.C.H. Steele, I. Kelly, H. Middleton, R. Rudkin, Solid State Ionics, 28–30 (1988) 1547.

[7] R. Ødegård, I.R. Theodorsen, T. Sigvartsen, T. Monsen, H. Løvåsen, Proc 14th Int. Mater. Sci., F.W. Poulsen, J.J. Bentzen, T. Jacobsen, E. Skou, M.J.L. Ostergard (Eds.), High Temp. Electrochem., Behaviour Fast Ion and Mixed Cond., Riso Nat. Lab., Denmark, 1993, p. 501.

[8] N.S. Jacobson, W.L. Worrell, Proc. High Temp. Mater. 2 (1983) 217.

[9] F.P.F. van Berkel, F.H. van Heuveln, J.P.P. Huijsmans, Solid State Ionics 72 (1993) 636.

[10] M. Mogensen, Proc 14th Int. Mater. Sci., F.W. Poulsen, J.J. Bentzen, T. Jacobsen, E. Skou, M.J.L. Ostergard (Eds.), High Temp. Electrochem., Behaviour Fast Ion and Mixed Cond., Riso Nat. Lab., Denmark, 1993, p. 117.

[11] F.M.B. Marques, G.P. Wirtz, J. Am. Ceram. Soc. 74 (1991) 598.

[12] F.M.B. Marques, G.P. Wirtz, J. Am. Ceram. Soc. 75 (1992) 369.

[13] F.M.B. Marques, G.P. Wirtz, J. Am. Ceram. Soc. 75 (1992) 375.

[14] H.G. Scott, J. Mater. Sci. 10 (1975) 1527.

[15] N.A. Bondar, L.N.K. Oroleva, N.A. Toropov, Izvestiya Akad. Nauk. SSSR, Neorg. Mater. 5 (1969) 1730.

[16] J.T.S. Irvine, I.R. Gibson, D.P. Fagg, Ionics 1 (1995) 279–285.

[17] J.T. Brown, in T. Takahashi (Ed.), High Conductivity Solid Ionic Conductors, Recent Trends and Applications, World Scientific, 1989, p. 630.